Med Chem Res
DOI 10.1007/s00044-013-0597-1

MEDICINAL CHEMISTRY RESEARCH

ORIGINAL RESEARCH

Synthesis, single-crystal, in vitro antitumor evaluation and molecular docking of 3-substitued 5,5-diphenylimidazolidine-2,4-dione derivatives

Amer M. Alanazi · Adel S. El-Azab · Ibrahim A. Al-Swaidan · Azza R. Maarouf · Eman R. El-Bendary · Mohamed A. Abu El-Enin · Alaa A.-M. Abdel-Aziz

Received: 4 November 2012 / Accepted: 24 April 2013

Abstract Series of 3-alkyl, 3-aryl-5,5-diphenylimidazolidine-2,4-diones (**2**–**8**) and 3-phenacyl-5,5-diphenylimidazolidine-2,4-diones (**9**–**20**) were designed, synthesized, and tested for their antitumor activity. The 13 compounds (**3**–**8**, **10**–**15** and **20**) were selected by National Cancer Institute (USA) on the basis of degree of the structure variation and computer modeling techniques for evaluation of their antineoplastic activity. A single dose (10 μM) of the tested compounds was used in the National Cancer Institute (NCI) 60 cell lines panel assay selected from different nine organs. The tested compounds possessed selective activity against the renal cancer (A498 and UO-31) cell lines. Interestingly, compound **13** showed moderate selective activities towards A498 and UO-31 cell lines, in addition to strong activity against melanoma (MDA-MB-435) cell line and breast cancer cell lines (MCF7) in 114 and 70 %, respectively. Molecular docking study was performed for the most active compound **13** to identify the structural features required for the antitumor activity. The results achieved can be used as a useful template for future development and further derivatization or modification to obtain more potent and selective antitumor agents.

A. M. Alanazi · A. S. El-Azab · I. A. Al-Swaidan · A. A.-M. Abdel-Aziz
Department of Pharmaceutical Chemistry, College of Pharmacy, King Saud University, Riyadh 11451, Saudi Arabia

A. S. El-Azab
Department of Organic Chemistry, Faculty of Pharmacy, Al-Azhar University, Cairo 11884, Egypt

A. R. Maarouf · E. R. El-Bendary · M. A. Abu El-Enin · A. A.-M. Abdel-Aziz (✉)
Department of Medicinal Chemistry, Faculty of Pharmacy, University of Mansoura, Mansoura 35516, Egypt
e-mail: alaa_moenes@yahoo.com

Keywords Cancer · Synthesis · Imidazolidine-2,4-dione · Antitumor · Molecular docking

Introduction

Cancer is continuing to be a major health problem worldwide and the leading cause of human mortality exceeded only by cardiovascular diseases (Lee *et al.*, 2002; Varmus, 2006; Avendaño and Menéndez, 2008; Eckhardt, 2002). The development of novel and efficient anticancer agents remains an important and challenging goal in medicinal chemistry (Lee *et al.*, 2002; Varmus, 2006; Avendaño and Menéndez, 2008; Eckhardt, 2002). Therefore, it is imperative to develop new anticancer drugs with more effective treatment strategies for cancer with well-defined pharmacokinetic properties (Abdel-Aziz *et al.*, 2012; Abdel-Aziz, 2007; Al-Obaid *et al.*, 2009; Al-Omary *et al.*, 2010; El-Azab *et al.*, 2010; El-Deeb *et al.*, 2010; El-Sherbeny *et al.*, 2010). During the last 10 years special attention of medicinal chemists was attracted by investigations of azolidinones as a potential lead compounds for novel anticancer agents (Abdel-Aziz *et al.*, 2012; El-Deeb *et al.*, 2010; Lee *et al.*, 2000; Kim *et al.*, 2003; Zuliani *et al.*, 2009; Penthala *et al.*, 2011; Thirupathi *et al.*, 2010; Basappa *et al.*, 2009; Khanfar and El Sayed, 2010; Ananda *et al.*, 2009; Carmi *et al.*, 2006; Cavazzoni *et al.*, 2008; Trišović *et al.*, 2011; Bakalova *et al.*, 2003). It is well documented that the important core fragment of azolidinones was defined by nitrogen heteroatomic system with at least of one carbonyl group and phenyl attached to the heterocyclic system (Abdel-Aziz *et al.*, 2012; El-Deeb *et al.*, 2010; Lee *et al.*, 2000; Kim *et al.*, 2003; Zuliani *et al.*, 2009; Penthala *et al.*, 2011; Thirupathi *et al.*, 2010; Basappa *et al.*, 2009; Khanfar and El Sayed, 2010; Ananda

Published online: 07 May 2013

et al., 2009; Carmi *et al.*, 2006; Cavazzoni *et al.*, 2008; Trišović *et al.*, 2011; Bakalova *et al.*, 2003). This common template was presented in the structures of two well established antitumor molecules such as imidazolidine-2-one (Abdel-Aziz *et al.*, 2012; Lee *et al.*, 2000; Kim *et al.*, 2003) and imidazolidine-2,4-dione (El-Deeb *et al.*, 2010; Zuliani *et al.*, 2009; Penthala *et al.*, 2011; Thirupathi *et al.*, 2010; Basappa *et al.*, 2009; Khanfar and El Sayed, 2010; Ananda *et al.*, 2009; Carmi *et al.*, 2006; Cavazzoni *et al.*, 2008; Trišović *et al.*, 2011; Bakalova *et al.*, 2003). Among the wide range of these compounds tested as potential anticancer agents, derivatives comprising the 5-(4-dimethylaminobenzylidene)-3-(4-chlorobenzenesulfonyl)imidazolidine-2,4-dione (**A**) (El-Deeb *et al.*, 2010), 1,3-bis (4-chlorobenzenesulfonyl)imidazolidine-2-one (**B**) (Abdel-Aziz *et al.*, 2012), 5,5-diphenylimidazolidine-2,4-dione (**C**) (Trišović *et al.*, 2011), and 3-phenethylimidazolidine-2,4-diones (**D**) (Zuliani *et al.*, 2009; Carmi *et al.*, 2006; Fig. 1).

Recently it was reported that the antitumor action and the inhibition of EGFR kinase activity by a series of 1,5-disubstituted imidazolidine-2,4-diones (Zuliani *et al.*, 2009; Carmi *et al.*, 2006; Cavazzoni *et al.*, 2008). These compounds were designed in view of the known interactions between 4-anilinoquinazolines, potent EGFR inhibitors, and the adenine binding portion of the ATP-binding site of the receptor (Traxler *et al.*, 1997; Wissner *et al.*, 2000; Bridges *et al.*, 1996). Molecular modeling showed that imidazolidine-2,4-dione could mimic the interactions of the quinazoline or 3-cyanoquinoline scaffolds with the hinge region of the EGFR ATP-binding site, accommodating an aromatic group at position C5 within the lipophilic pocket occupied by the 4-anilino one in the EGFR-erlotinib co-crystal. The resulting 5-benzylidene imidazolidine-2,4-dione inhibited the EGFR kinase and exhibited a cytotoxic action on A431 human epidermoid carcinoma cells (Zuliani *et al.*, 2009; Carmi *et al.*, 2006; Cavazzoni *et al.*, 2008).

Taking into consideration the above mentioned findings our researches have focused on systematic structural modifications in a group of imidazolidine-2-one and imidazolidine-2,4-dione derivatives (Abdel-Aziz *et al.*, 2012; El-Deeb *et al.*, 2010; Lee *et al.*, 2000; Kim *et al.*, 2003; Zuliani *et al.*, 2009; Penthala *et al.*, 2011; Thirupathi *et al.*, 2010; Basappa *et al.*, 2009; Khanfar and El Sayed, 2010; Ananda *et al.*, 2009; Carmi *et al.*, 2006; Cavazzoni *et al.*, 2008; Trišović *et al.*, 2011; Bakalova *et al.*, 2003). Structure–activity relationships (SARs) study performed among these molecules showed higher activity for differently substituted imidazolidine-2,4-diones in comparison to respective imidazolidine-2-one analogs. Following these findings as a part of our efforts to design new antitumor agents in the present studies, we have synthesized a new series of 3-substituted 5,5-diphenylimidazolidine-2,4-diones (**E**, Fig. 1). These molecules have been designed as analogs of compounds **A** and **C** (Fig. 1) in which phenacyl moiety containing basic fragments was incorporated basically as a part of the cyclic structures of imidazolidine-2,4-diones because of the reported potential antitumor activity of this ring system. To the best of our knowledge, there are no reports concerning antitumor activity for phenacylimidazolidine-2,4-diones were reported. Molecular modeling studies are required in order to construct molecular models that incorporate all experimental evidence reported (Abdel-Aziz *et al.*, 2011, 2010; Abdel-Aziz, 2007; Al-Obaid *et al.*, 2009; Al-Omary *et al.*, 2010; El-Azab *et al.*, 2010; El-Deeb *et al.*, 2010; El-Sherbeny *et al.*, 2010; El-Sayed *et al.*, 2012, 2011; El-Ayaan *et al.*, 2007; Goda *et al.*, 2005). These models are necessary to obtain a consistent and more precise picture of the biological active molecules at the atomic level and provide furthermore new insights that can be used to design novel therapeutic agents.

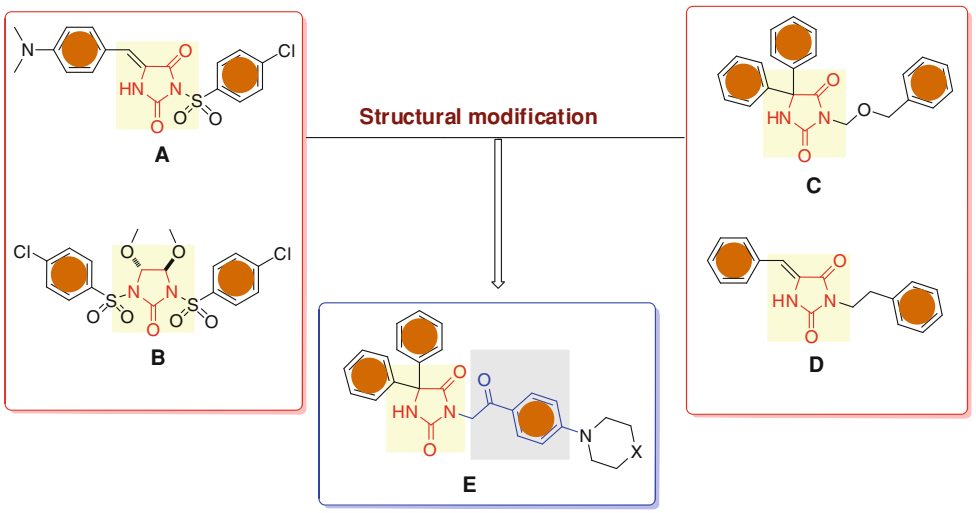

Fig. 1 Examples of reported structure lead compounds among imidazolidine (**a**–**d**) with anticancer properties and designed imidazolidine-2,4-diones (**e**)

Materials and methods

Chemistry

Melting points (uncorrected) were recorded on Barnstead 9100 Electrothermal melting apparatus. IR spectra were recorded on a FT-IR Perkin-Elmer spectrometer. ^{1}H NMR and ^{13}C NMR were recorded in DMSO-d_6 and/or $CDCl_3$ on a Bruker 500 MHz instrument using TMS as internal standard (chemical shifts in δ ppm). Mass spectra were recorded on on a Perkin-Elmer, Clarus 600T GC/MS, and Varian, TQ 320 GC/MS/MS mass spectrometers. Solvent evaporation was performed under reduced pressure using Buchan Rotatory Evaporator unless otherwise stated. Thin layer chromatography was performed on precoated (0.25 mm) silica gel GF_{254} plates (E. Merck, Germany), compounds were detected with 254 nm UV lamp. Silica gel (60–230 mesh) was employed for routine column chromatography separations. The well-known compounds **2–5** and **7–8** were prepared following the procedures reported in the literature (Ooms *et al.*, 2002; Dumbris *et al.*, 2009; Hmuda *et al.*, 2011; El-Zanfally *et al.*, 1968; Peretto *et al.*, 2007).

*Synthesis of 2-(3-(2,5-dioxo-4,4-diphenylimidazolidin-1-yl)propyl)isoindoline-1,3-dione (**6**)*

A mixture of compound **1** (0.01 mol) and K_2CO_3 (0.01 mol) was stirred in DMF at room temperature for 20 min. To the reaction mixture, a solution of the 2-(3-bromopropyl)isoindoline-1,3-dione (0.011 mol) in DMF was added dropwise over a period of 10 min. The resulted mixture was further stirred for 24 h at room temperature. The separated solid was then filtered, washed with cold water, dried and crystallized from CH_2Cl_2.

White powder, MP 190–192 °C, 87 % yield (CH_2Cl_2); (KBr, cm^{-1}) *v*: 3272 (NH), 1771, 1703 (C=O); ^{1}H NMR ($CDCl_3$): δ 7.84 (t, 2H, $J = 4.0$ Hz), 7.72 (s, 2H), 7.38–7.36 (m, 10H), 6.87 (s, 1H), 3.75 (t, 2H, $J = 7.0$ Hz), 3.67 (t, 2H, $J = 7.0$ Hz), 2.08 (t, 2H, $J = 7.0$ Hz); ^{13}C NMR ($CDCl_3$): δ 173.2, 168.1, 156.3, 139.0, 133.9, 132.0, 128.8, 128.6, 126.9, 123.3, 70.1, 36.8, 35.5, 27.4; $C_{26}H_{21}N_3O_4$: *m/z* (439.0).

*General procedure for synthesis of compounds **9–12***

A mixture of compound **1** (0.01 mol) and K_2CO_3 (0.01 mol) was stirred in acetone at room temperature for 20 min. To the reaction mixture, a solution of the phenacyl chloride (0.011 mol) in acetone was added dropwise over a period of 20 min. The resulted mixture was further stirred for 24 h at room temperature. The separated solid was then filtered, washed with cold water, dried and crystallized from an appropriate solvent.

*3-(2-Oxo-2-phenylethyl)-5,5-diphenylimidazolidine-2,4-dione (**9**)*

White crystals, MP 233–235 °C, 91 % yield (CH_2Cl_2/Hexane); IR (KBr, cm^{-1}) *v*: 3293 (NH), 1775, 1705, 1694 (C=O); ^{1}H NMR (DMSO-d_6): δ 9.50 (s, 1H, NH), 8.08–8 (d, 2H, $J = 7.0$ Hz), 7.74 (t, 1H, $J = 7.0$ Hz), 7.61 (t, 2H, $J = 7.5$ Hz), 7.45-7.39 (m, 10H), 5.08 (s, 2H); ^{13}C NMR (DMSO-d_6): δ 192.1, 173.4, 154.9, 139.5, 134.2, 133.9, 128.9, 128.5, 128.2, 128.1, 127.5, 126.8, 69.7, 44.8; $C_{23}H_{18}N_2O_3$: *m/z* (370.0).

*3-(2-(4-Chlorophenyl)-2-oxoethyl)-5,5-diphenylimidazolidine-2,4-dione (**10**)*

White crystals, MP 245–246 °C, 95 % yield (CH_2Cl_2); IR (KBr, cm^{-1}) *v*: 3299 (NH), 1770, 1702, 1691 (C=O); ^{1}H NMR (DMSO-d_6): δ 9.30 (s, 1H), 7.43–7.27 (m, 5H), 7.22–7.00 (m, 5H), 6.96 (d, 2H, $J = 7.0$ Hz), 7.48 (d, 2H, $J = 7.0$ Hz), 5.11 (s, 2H); ^{13}C NMR (DMSO-d_6): δ 189.1, 172.6, 154.7, 152.8, 139.7, 138.7, 136.2, 134.3, 129.8, 128.6, 128.0, 127.5, 126.5, 126.4, 124.7, 69.0, 40.1; $C_{23}H_{17}ClN_2O_3$: *m/z* (404.0).

*3-(2-(4-Fluorophenyl)-2-oxoethyl)-5,5-diphenylimidazolidine-2,4-dione (**11**)*

White crystals, MP 259–260 °C, 96 % yield (MeOH); IR (KBr, cm^{-1}) *v*: 3297 (NH), 1768, 1700, 1699 (C=O); ^{1}H NMR (DMSO-d_6): δ 9.78 (s, 1H, NH), 8.18–8.15 (q, 2H, $J = 7.5$ Hz), 7.47–7.39 (m, 12H), 5.08 (s, 2H); ^{13}C NMR (DMSO-d_6): δ 190.8, 173.3, 166.5, 164.5, 154.8, 139.5, 131.3, 131.3, 130.7, 128.5, 128.2, 126.8, 126.5, 116.1, 116.0, 62.9, 44.7; $C_{23}H_{17}FN_2O_3$: *m/z* (388.3).

*3-(2-(4-Methoxypehnyl)-2-oxoethyl)-5,5-diphenylimidazolidine-2,4-dione (**12**)*

White powder, MP 285–286 °C, 78 % yield (MeOH); IR (KBr, cm^{-1}) *v*: 3237 (NH), 1779, 1706 (C=O); ^{1}H NMR (DMSO-d_6): δ 9.20 (s, 1H), 7.62 (2, 2H, $J = 7.0$ Hz), 7.45–7.38 (m, 12H), 5.20 (s, 2H), 3.71 (s, 3H); ^{13}C NMR (DMSO-d_6): δ 190.0, 173.5, 155.0, 140.0, 134.9, 134.3, 129.3, 128.9, 128.6, 128.5, 127.4, 126.0, 68.5, 49.0, 44.8; $C_{24}H_{20}N_2O_4$: *m/z* (400.0).

*General procedure for synthesis of compounds **13–20***

A mixture of compound **11** (0.01 mol), K_2CO-$_3$ (0.02 mol) and secondary amine (0.01 mol) were stirred in DMSO (10 mL) at 80 °C for 6 h. The resulted mixture was then cooled and poured into crushed ice. The separated solid

was then filtered, washed with cold water, dried and purified by column chromatography.

*3-(2-Oxo-2-(4-(piperidin-1-yl)phenyl)ethyl)-5,5-diphenylimidazolidine-2,4-dione (**13**)*

Yellow crystals, MP 265–266 °C, 69 % yield (CH_2Cl_2); IR (KBr, cm^{-1}) *v*: 3177 (NH), 1775, 1719, 1676 (C=O); ^{1}H NMR (DMSO-d_6): δ 7.78 (d, 2H, $J = 9.0$ Hz), 7.42 (d, 4H, $J = 7.0$ Hz), 7.30–7.26 (m, 6H), 6.78 (s, 2H), 6.62 (s, 1H), 4.84 (s, 2H), 3.30 (s, 4H), 1.59 (s, 6H); ^{13}C NMR (DMSO-d_6): δ 188.0, 173.7, 156.1, 154.6, 139.1, 130.3, 128.7, 128.5, 127.3, 123.4, 113.2, 70.8, 48.4, 44.4, 25.2, 24.3; $C_{28}H_{27}N_3O_3$: *m/z* (453.5).

*3-(2-(4-Morpholinophenyl)-2-oxoethyl)-5,5-diphenylimidazolidine-2,4-dione (**14**)*

Yellow crystals, MP 271–272 °C, 61 % yield (CH_2Cl_2); IR (KBr, cm^{-1}) *v*: 3176 (NH), 1774, 1717, 1678 (C=O); ^{1}H NMR (DMSO-d_6): δ 8.97 (d, 1H, $J = 10$ Hz), 7.41 (d, 2H, $J = 8.0$ Hz), 7.03 (d, 4H, $J = 7.0$ Hz), 6.91–6.86 (m, 6H), 6.44 (d, 2H, $J = 8.5$ Hz), 4.41 (s, 2H), 2.85 (s, 4H), 2.72 (s, 4H); ^{13}C NMR (DMSO-d_6): δ 188.5, 173.5, 155.1, 154.2, 139.3, 129.6, 128.0, 127.7, 126.9, 123.9, 112.7, 69.8, 65.8, 46.6, 43.8; $C_{27}H_{25}N_3O_4$: *m/z* (455.5).

*3-(2-(4-(4-Phenylpiperidin-1-yl)phenyl)-2-oxoethyl)-5,5-diphenylimidazolidine-2,4-dione (**15**)*

White powder, MP 187–189 °C, 73 % yield (CH_2Cl_2); IR (KBr, cm^{-1}) *v*: 3175 (NH), 1775, 1716, 1676 (C=O); ^{1}H NMR (DMSO-d_6): δ 7.78 (d, 2H, $J = 9.0$ Hz), 7.39-7.34 (m, 6H), 7.30–7.26 (m, 9H), 7.02 (d, 2H, $J = 7.5$ Hz), 6.85 (s, 1H), 4.79 (s, 2H), 3.80 (d, 2H, $J = 13.5$ Hz), 2.75 (t, 2H, $J = 12.0$ Hz), 2.46 (d, 2H, $J = 7.5$ Hz), 1.70 (q, 3H, $J = 13.5$ Hz); ^{13}C NMR (DMSO-d_6): δ 188.0, 173.7, 156.2, 154.4, 139.8, 130.5, 128.9, 128.6, 128.2, 122.9, 123.2, 113.3, 70.8, 53.1, 48.1, 44.5, 43.8, 38.6; $C_{34}H_{31}N_3O_3$: *m/z* (529.0).

*3-(2-(4-(4-Benzylpiperidin-1-yl)phenyl)-2-oxoethyl)-5,5-diphenylimidazolidine-2,4-dione (**16**)*

Yellow powder, MP 133–135 °C, 66 % yield (CH_2Cl_2); IR (KBr, cm^{-1}) *v*: 3220 (NH), 1774, 1716, 1675 (C=O); ^{1}H NMR (DMSO-d_6): δ 7.76 (d, 2H, $J = 9.0$ Hz), 7.41 (d, 4H, $J = 7.0$ Hz), 7.29–7.19 (m, 8H), 7.15–7.10 (m, 1H), 7.07 (d, 2H, $J = 7.0$ Hz), 6.86 (s, 1H), 6.75 (d, 2H, $J = 8.0$ Hz), 5.18 (s, 2H), 4.78 (s, 2H), 3.81 (d, 2H, $J = 13.0$ Hz), 2.76 (t, 2H, $J = 12.5$ Hz), 2.48 (d, 2H, $J = 7.0$ Hz), 1.69 (q, 3H, $J = 13.5$ Hz); ^{13}C NMR (DMSO-d_6): δ 188.0, 173.7, 156.2, 154.4, 140.1, 139.1, 130.3, 129.1, 128.7, 128.33, 127.3, 126.0, 123.5, 113.3, 70.8, 53.4, 47.7, 44.4, 43.0, 38.0, 31.4; $C_{35}H_{33}N_3O_3$: *m/z* (543.6).

*3-(2-Oxo-2-(4-(4-phenylpiperazin-1-yl)phenyl)ethyl)-5,5-diphenylimidazolidine-2,4-dione (**17**)*

Yellow powder, MP 259–260 °C, 59 % yield (MeOH); IR (KBr, cm^{-1}) *v*: 3214 (NH), 1777, 1715, 1673 (C=O); ^{1}H NMR (DMSO-d_6): δ 8.14 (s, 1H), 7.83 (d, 2H, $J = 9.0$ Hz), 7.45–7.37 (m, 6H), 7.33–7.28 (m, 6H), 6.83 (d, 2H, $J = 9.0$ Hz), 6.62 (d, 2H, $J = 7.0$ Hz), 6.22 (s, 1H), 4.84 (s, 2H), 3.66 (s, 4H), 3.46 (s, 4H); ^{13}C NMR (DMSO-d_6): δ 188.2, 173.6, 155.9, 154.3, 139.0, 130.2, 128.7, 128.6, 127.3, 124.4, 113.7, 113.2, 70.8, 63.4, 46.6, 44.7, 44.5; $C_{33}H_{30}N_4O_3$: *m/z* (529.8).

*3-(2-(4-(4-(2-Ethoxyphenyl)piperazin-1-yl)phenyl)-2-oxoethyl)-5,5-diphenylimidazolidine-2,4-dione (**18**)*

Yellow powder, MP 167–168 °C, 55 % yield (MeOH); IR (KBr, cm^{-1}) *v*: 3170 (NH), 1773, 1711, 1670 (C=O); ^{1}H NMR (DMSO-d_6): δ 7.83 (d, 2H, $J = 9.0$ Hz), 7.43 (d, 4H, $J = 6.5$ Hz), 7.32–7.27 (m, 6H), 6.93 (s, 1H), 6.86–6.80 (m, 5H), 6.51 (s, 1H), 4.83 (s, 2H), 4.02 (t, 2H, $J = 7.0$ Hz), 3.47 (s, 4H), 3.15 (s, 4H), 1.40 (s, 3H); ^{13}C NMR (DMSO-d_6): δ 188.2, 173.7, 156.0, 154.7, 151.6, 140.8, 139.1, 130.2, 128.7, 128.5, 127.3, 124.4, 123.2, 121.0, 118.2, 113.4, 112.6, 70.8, 63.7, 50.3, 47.4, 44.5, 14.9; $C_{35}H_{34}N_4O_4$: *m/z* (574.6).

*3-(2-(4-(4-(2-Chlorophenyl)piperazin-1-yl)phenyl)-2-oxoethyl)-5,5-diphenylimidazolidine-2,4-dione (**19**)*

Yellow powder, MP 216–218 °C, 57 % yield (MeOH); IR (KBr, cm^{-1}) *v*: 3089 (NH), 1773, 1717, 1672 (C=O); ^{1}H NMR (DMSO-d_6): δ 9.70 (s, 1H), 7.94 (d, 2H, $J = 8.5$ Hz), 7.45–7.38 (m, 11H), 7.33 (t, 1H, $J = 7.0$ Hz), 7.19 (d, 1H, $J = 7.0$ Hz), 7.08 (t, 3H, $J = 8.0$ Hz), 4.93 (s, 2H), 3.54 (s, 4H), 3.11 (s, 4H); ^{13}C NMR (DMSO-d_6): δ 189.2, 173.5, 155.1, 154.3, 148.5, 139.6, 130.3, 130.1, 128.4, 128.2, 128.1, 127.6, 126.9, 124.2, 123.4, 120.9, 113.1, 69.6, 56.0, 50.5, 46.6, 44.2; $C_{33}H_{29}ClN_4O_3$: *m/z* (565.0).

*3-(2-(4-(4-(4-Chlorophenyl)piperazin-1-yl)phenyl)-2-oxoethyl)-5,5-diphenylimidazolidine-2,4-dione (**20**)*

Yellow powder, MP 277–279 °C, 57 % yield (MeOH); IR (KBr, cm^{-1}) *v*: 3231 (NH), 1774, 1716, 1674 (C=O); ^{1}H NMR (DMSO-d_6): δ 9.73 (s, 1H), 7.93 (d, 2H, $J = 9.0$ Hz), 7.43–7.38 (m, 10H), 7.27 (d, 2H, $J = 9.0$ Hz), 7.08 (d, 2H, $J = 8.5$ Hz), 6.99 (s, 2H), 4.92

Scheme 1 Synthesis of 3-substituted imidazolidine-2,4-diones (**2**–**12**)

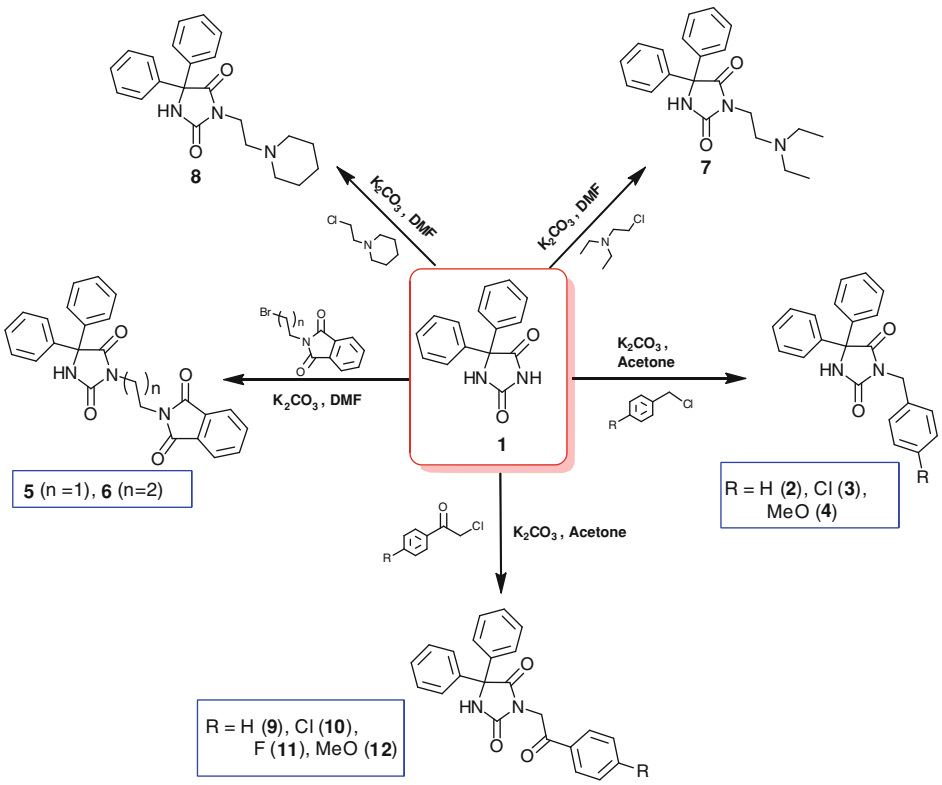

Scheme 2 Synthesis of substituted 3-phenacylimidazolidine-2,4-diones (**13**–**20**)

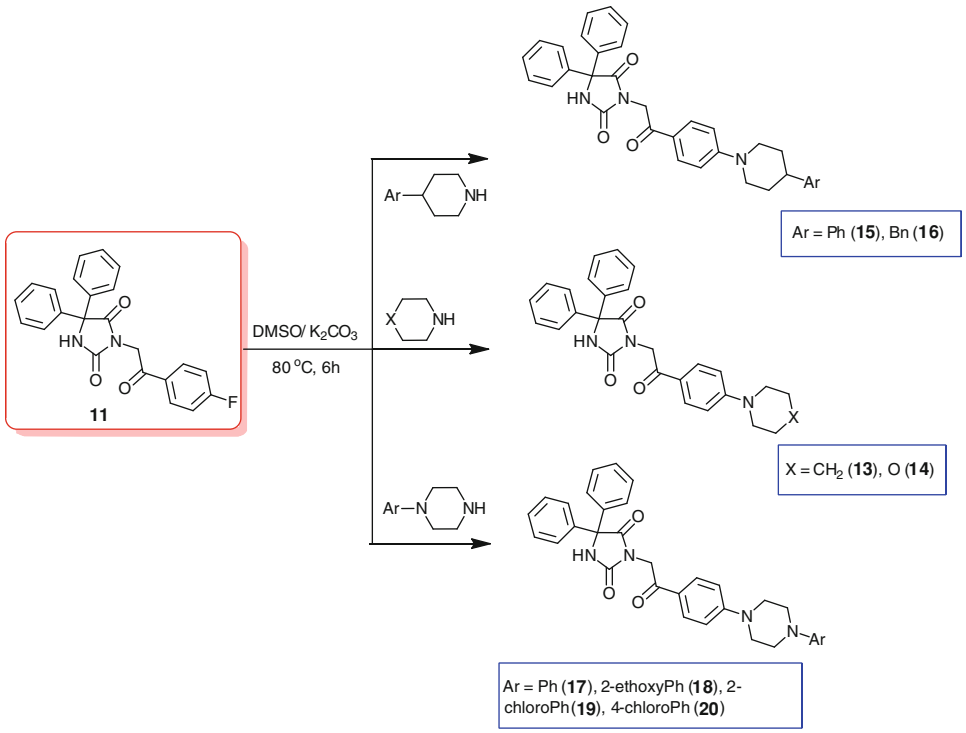

(s, 2H), 3.54 (s, 3H), 3.29 (s, 5H); ^{13}C NMR (DMSO-d_6): δ 189.1, 173.5, 155.0, 154.0, 149.4, 139.5, 130.1, 128.6, 128.4, 128.2, 126.9, 123.3, 122.6, 116.9, 113.1, 69.6, 62.9, 47.6, 46.0, 44.2; $C_{33}H_{29}ClN_4O_3$: *m*/*z* (565.0).

Antitumor methodology

The human tumor cell lines of the cancer screening panel are grown in RPMI 1640 medium containing 5 % fetal

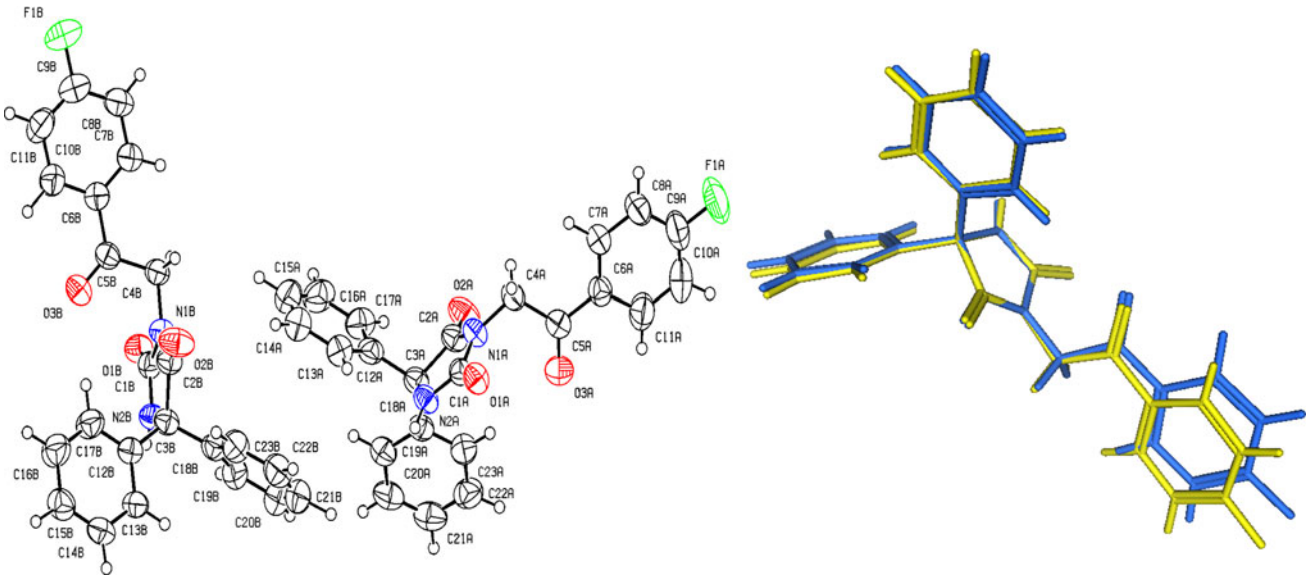

Fig. 2 X-ray crystal structure and numbering system of compound **11** (*left panel*), *right panel* showed overlay of two conformers

bovine serum and 2.0 mM L-glutamine. For a typical screening experiment, cells are inoculated into 96-well microtiter plates in 100 µL at plating densities ranging from 5,000 to 40,000 cells/well depending on the doubling time of individual cell lines. After cell inoculation, the microtiter plates are incubated at 37 °C, 5 % CO_2, 95 % air and 100 % relative humidity for 24 h prior to addition of experimental drugs. After 24 h, two plates of each cell line are fixed in situ with trichloroacetic acid (TCA), to represent a measurement of the cell population for each cell line at the time of drug addition (*Tz*). Experimental drugs are solubilized in dimethyl sulfoxide at 400-fold the desired final maximum test concentration and stored frozen prior to use. At the time of drug addition, an aliquot of frozen concentrate is thawed and diluted to twice the desired final maximum test concentration with complete medium containing 50 µg/ml gentamicin. Aliquot of 100 µl of this drug dilution was added to the appropriate microtiter wells already containing 100 µl of medium, resulting in the required final drug concentrations. Following drug addition, the plates are incubated for an additional 48 h at 37 °C, 5 % CO_2, 95 % air, and 100 % relative humidity. For adherent cells, the assay is terminated by the addition of cold TCA. Cells are fixed in situ by the gentle addition of 50 µl of cold 50 % (w/v) TCA (final concentration, 10 % TCA) and incubated for 60 min at 4 °C. The supernatant is discarded, and the plates are washed five times with tap water and air dried. Sulforhodamine B (SRB) solution (100 µl) at 0.4 % (w/v) in 1 % acetic acid is added to each well, and plates are incubated for 10 min at room temperature. After staining, unbound dye is removed by washing five times with 1 % acetic acid and the plates are air dried. Bound stain is subsequently solubilized with 10 mM trizma base, and the absorbance is read on an automated plate reader at a wavelength of 515 nm. For suspension cells, the methodology is the same except that the assay is terminated by fixing settled cells at the bottom of the wells by gently adding 50 µl of 80 % TCA (final concentration, 16 % TCA) (Grever *et al.*, 1992; Monks *et al.*, 1991; Boyd and Paull, 1995).

Docking methodology

Docking studies have been performed using MOE 2008.10 (2008). Docking procedure was followed using the standard protocol implemented in MOE 2008.10 and the geometry of resulting complexes was studied using the MOE's Pose Viewer utility.

Results and discussion

Chemistry

Scheme 1 outlines the synthetic pathway used to obtain compounds (**2–12**) (Ooms *et al.*, 2002; Dumbris *et al.*, 2009; Hmuda *et al.*, 2011; El-Zanfally *et al.*, 1968; Peretto *et al.*, 2007). The starting material 5,5-diphenylimidazolidine-2,4-diones (**1**) was reacted with an appropriate alkyl chloride in the presence of K_2CO_3 using acetone or DMF as a solvent to afford 3-substituted 5,5-diphenylimidazolidine-2,4-diones (**2–12**) in a relatively good yield. Compound **11** was reacted with an appropriate secondary amine in DMSO using K_2CO_3 as a base to afford the

Table 1 Summary of crystal data, data collection, and structure refinement for compound **11**

A. Crystal data	
Empirical formula	$C_{23}H_{17}FN_2O_3$
Formula weight	388.39
Crystal color, habit	Colorless, crystals
Space group hall symbol	P 2c -2ac
Space group H-M symbol	P c a 2_1
Crystal system	Orthorhombic
Lattice parameters	$a = 19.9930(10)$ Å
	$b = 8.1101(4)$ Å
	$c = 23.2644(12)$ Å
	$\alpha = 90.0°$
	$\beta = 90.0°$
	$\gamma = 90.0°$
Z value	8
Cell volume (V)	3,772.21 (3) $Å^3$
R-Factor (%)	3.67
D_{calc}	1.368 gm cm^3
F_{000}	1,616.0
μ (Cu Kα)	0.813 11 mm^{-1}
Cu $K\alpha$ radiation, λ	1.54178 cm^{-1}
T	296 K
B. Data collection and refinement	
Diffractometer	Bruker SMART APEXII CCD
Structure solution	Direct methods
Radiation	Cu Kα ($\lambda = 1.54178$ Å)
	Graphite monochromated
Radiation source	Fine-focus sealed tube
$2\theta_{max}$	69.770°
No. of reflections measured	Total: 5,132
	Unique: 3,659 ($R_{int} = 0.0367$)
Corrections	Lorentz-polarization
	Absorption
Refinement	Full-matrix least-squares
Residuals: Rw	0.1117
Goodness of fit indicator	0.845

3-(4-substituted phenacyl)-5,5-diphenylimidazolidine-2,4-diones (**13–20**) in satisfactory yields (Scheme 2). All of the obtained new compounds **7** and **9–20** were identified on the basis of the analytical data. The ^{1}H NMR spectra of the prepared imidazolidine-2,4-diones have shown that only 3-substituted derivatives were obtained, and its regioisomer 1-substituted derivatives could not be formed at this study which was confirmed by measuring the X-ray crystallography (Fig. 2) of compound **11**.

The molecular solid state structure and numbering system of compound **11** are indicated in Fig. 2. Compound **11** crystallized with $Z = 8$ in the space group $Pca2_1$ with two independent molecules (A and B) in the asymmetric unit (Table 1; Fig. 2). It is composed of 5,5-diphenylimidazolidine-2,4-dione moiety substituted with a *p*-fluorophenacyl group. Both molecules are extended-shaped with a similar geometry of 5,5-diphenylimidazolidine-2,4-dione and different conformation of the *p*-fluorophenacyl group as it can be seen by the Auto-Fit diagram (Fig. 2, right panel). Both 5-phenyl groups are orthogonal and the phenacyl moiety is stabilized in an extended conformation. In the crystal structure, the molecules are connected via N–H···O hydrogen bonds. Crystal structure determination of **11** (Fig. 2) was carried out in order to elucidate its structural properties, the potential functional groups interacting with the target, and give a stable conformation useful for docking studies.

In vitro antitumor evaluation and structure–activity relationship

The 13 compounds were selected by National Cancer Institute, Bethesda, Maryland, USA (Figs. 3, 4; Tables 2, 3) on the basis of degree of the structure variation and computer modeling techniques for evaluation of their antineoplastic activity (Grever *et al.*, 1992; Monks *et al.*, 1991; Boyd and Paull, 1995). The selected compounds were subjected to in vitro anticancer assay against tumor cells in a full panel of 60-cell lines taken from 9 different organs (lung, colon, breast, ovary, blood, kidney, skin, prostate, and brain). The compounds were tested at a single dose concentration of 10 μM, the percentages of growth inhibitions over the 60 tested cell lines were determined and the results were compared with compounds **A** and **B** (Abdel-Aziz *et al.*, 2012; El-Deeb *et al.*, 2010). The percentages of growth inhibitions over the most sensitive 10-cell lines are shown in Table 2 and Fig. 3.

By investigating the variation in selectivity of the tested compounds over the full panel of cell lines, it was revealed that nearly all of the compounds under investigation showed significant inhibition for the renal cell lines (A498 and UO-31). The percentages of inhibition for renal cancer cell (A498) reached to more than 50 % in a number of the tested derivatives (Table 2; Fig. 3). However, distinguish in selectivity was observed between the first series **2–8**, and the second series **9–20**. In the first series **2–8**, a significant inhibition for renal cancer cells (A498 and UO-31; 18–58 %) was observed, while the other series **9–20**, shows a significant inhibition for renal cancer cells (A498 and UO-31; 37–68 %), leukemia cancer cell (K-562; 27–50 %), non-small lung cancer cells (HOP-92 and NCI-H522; 14–66 %), melanoma cancer cells (M14 and MDA-MB-435; 57–114 %), breast cancer (MCF7; 10–70 %). The agreement between the two series in the inhibition of renal cell line (A498 and UO-31) cells could be correlated to a similar inhibitory mechanism related to the common

Table 2 The percentages of growth inhibition of the 13 selected compounds over the most sensitive tumor cell lines

Comp. no.	K-562 (%)	HOP-92 (%)	NCI-H522 (%)	HCT-15 (%)	M14 (%)	MDA-MB-435 (%)	A498 (%)	UO-31 (%)	MCF7 (%)	PC-3 (%)
3	–	–	18.02	16.12	9.44	1.11	58.66	35.82	9.14	22.07
4	–	46.99	6.58	20.51	12.03	–	35.89	31.31	7.44	22.21
5	–	–	−2.36	3.23	4.46	1.11	18.73	20.44	1.85	4.50
6	–	–	−7.36	−3.05	1.28	−3.96	42.46	31.56	−1.93	1.01
7	1.14	2.13	−0.51	−12.40	−8.75	−5.57	35.42	20.81	–	5.41
8	3.38	−5.79	−10.89	–	−7.37	−3.47	53.76	25.11	2.96	−2.57
10	–	–	12.57	6.41	14.33	5.55	43.06	35.49	20.09	49.31
11	–	–	3.09	–	8.32	1.89	55.23	26.66	4.32	4.43
12	–	28.50	3.51	0.5	−3.57	−3.01	29.53	28.76	–	5.04
13	50.22	66.24	55.49	55.25	57.09	114.20	68.14	53.43	70.51	28.21
14	6.02	2.32	24.82	1.67	−9.07	–	–	47.75	7.24	20.30
15	–	0.17	29.55	16.68	−8.35	–	–	41.04	12.96	6.88
20	27.55	22.24	14.44	17.14	10.71	6.47	−6.05	37.35	10.07	26.35
A[a]	8.89	11.19	9.78	1.55	199.62	−4.89	−8.94	5.5	−6.37	−6.65
B[b]	23.23	49.89	26.66	19.75	6.23	–	4.59	39.39	16.02	29.78

The showed inhibition percentages are measured at a single concentration of 10 μM

[a,b] Data was taken from El-Deeb *et al.* (2010) and Abdel-Aziz *et al.* (2012)

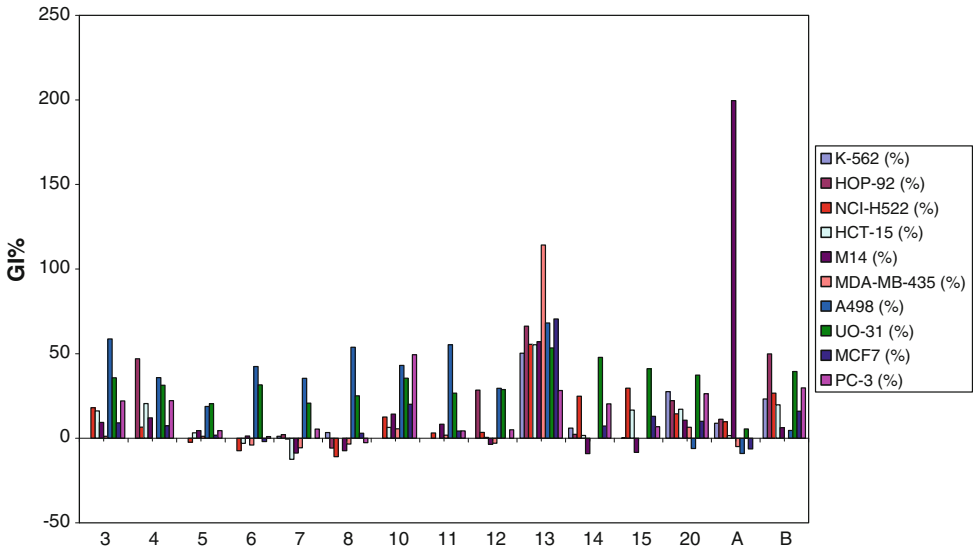

Fig. 3 The percentages of growth inhibition of the 13 selected compounds and reference compounds (**a**, **b**) over the most sensitive tumor cell lines

structural feature in the two series (5,5-diphenyl-2,4-imidazolidinedione core), while the variation in selectivity over melanoma cancer cells (M14, MDA-MB-435) and breast cancer (MCF7) is probably caused by the differences in the hydrocarbon and heterocyclic skeleton around the core structure (5,5-diphenyl-2,4-imidazolidinedione) in the two series at 3 position, where phenacyl moieties showed higher activity compared with benzyl, alkyl imides and alkyl nitrogen fragments. More interestingly compound **13** (Table 3; Fig. 4), showed broad spectrum activity against different cell lines including renal cancer cells (A498 and UO-31; 68 and 53 %, respectively), leukemia cancer cell (K-562; 50 %), non-small lung cancer cells (HOP-92 and NCI-H522; 66 and 55 %, respectively). Moreover great inhibitions of compound **13** for both MCF7 breast cancer and MDA-MB-435 melanoma cancer cells (70 % and 114 %, respectively) were observed at the tested concentration (10 μM). This great inhibition at the mentioned concentration indicates a great potency for the compound **13** with a strong lethal effect over breast cancer (MCF7) and melanoma (MDA-MB-435) cells. These results indicate the importance of the unsubstituted basic piperidine fragment at certain distance from imidazolidine-2,4-dione core as compared to compound **8**. The lower activity of

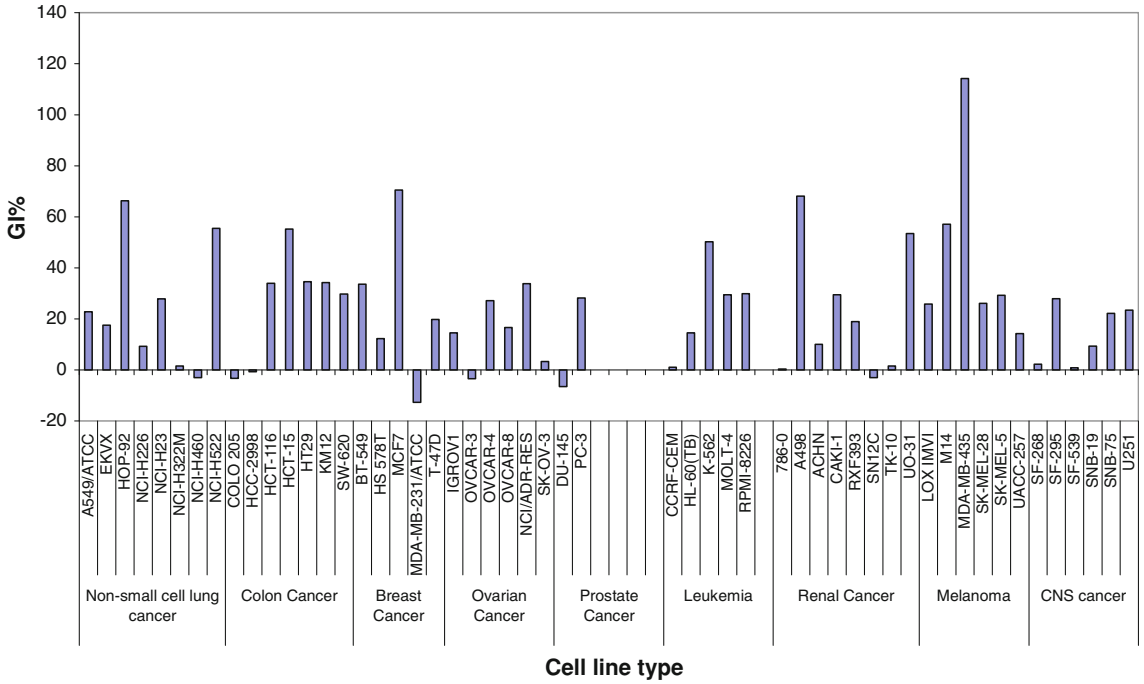

Fig. 4 The percentages of growth inhibition of compound **13** over the full panel of tumor cell lines

compound **15** may be attributed to its physicochemical properties as can be seen in Table 4. Moreover piperidine fragment showed higher activity when compared with morpholine analog **14** which may be attributed to its higher basic character compared with morpholine ring system. According to the antitumor activity results and structural variation, the minimal structural requirements for antitumor activity are as follows; two aromatic rings separated by an average distance, a basic nitrogen atom separated from the imidazolidione-2,4-dione core by certain distance, a hydrophobic moiety directly attached to the basic centre, and a H-bonding acceptor (carbonyl group) attached to H-donor urea fragment. This pharmacophoric postulation was in consistence with the reported results for other antitumor azolidine pharmacophore (Abdel-Aziz *et al.*, 2012; El-Deeb *et al.*, 2010; Kim *et al.*, 2003; Zuliani *et al.*, 2009; Carmi *et al.*, 2006; Park Choo *et al.*, 2001; Choo *et al.*, 2003).

Lipinski rule of five and molecular docking studies

As a part of our study; the compliance of compounds to the Lipinski's rule of five was evaluated (Lipinski *et al.*, 2001). Briefly, this simple rule is based on the observation that most biological active drugs have a molecular weight (MW) of 500 or less, a logP not higher than 5, five or fewer hydrogen bond donor sites and ten or fewer hydrogen bond acceptor sites. In addition, the polar surface area (PSA) of the compounds was also calculated (Table 4), since it is another key property that has been linked to drug bioavailability, where passively absorbed compounds with a PSA > 140 Å^2 are thought to have low oral bioavailability (Clark and Pickett, 2000). The results disclosed in Table 4 show that most of the tested compounds comply with these rules. Hence; theoretically, most of these compounds should present good passive oral absorption and differences in their bioactivity cannot be attributed to this property. Although lipophilicity does not exert a significant effect on activity in tested compounds, an increase in potency was observed in compounds **3–13** with logP in range of 3.2–4.58. It is clear that the lipophilicity of molecules is not the principal factor that determines their activity.

The level of antitumor activities of the compound **13** over breast cancer (MCF-7) and melanoma cancer (M14, MDA-MB-435) cells, in which epidermal growth factor receptor (EGFR) and GG V600E-B-RAF kinase is highly expressed, respectively (Fricker, 2006; Madhusudan and Ganesan, 2004; Cockerill and Lackey, 2002; Brose *et al.*, 2002), prompted us to perform molecular docking into the ATP binding site of EGFR and V600E-B-RAF kinase to predict if this compound **13** has analogous binding mode to the EGFR and V600E-B-RAF kinase inhibitors. We assumed that the active target compound **13** might demonstrate antiproliferative activity against breast cancer (MCF-7) and melanoma cancer (M14, MDA-MB-435) cell lines through inhibition of EGFR and V600E-B-RAF, respectively.

Table 3 The percentages of growth inhibition of compound **13** over the full panel of tumor cell lines

Cell line type	Cell line name	Inhibition (%)
Non-small cell lung cancer	A549/ATCC	22.82
	EKVX	17.56
	HOP-92	66.24
	NCI-H226	9.28
	NCI-H23	27.82
	NCI-H322 M	1.59
	NCI-H460	−2.99
	NCI-H522	55.49
Colon cancer	COLO 205	−3.28
	HCC-2998	−0.70
	HCT-116	33.97
	HCT-15	55.25
	HT29	34.66
	KM12	34.22
	SW-620	29.78
Breast cancer	BT-549	33.60
	HS 578T	12.31
	MCF7	70.51
	MDA-MB-231/ATCC	−12.67
	T-47D	19.80
Ovarian cancer	IGROV1	14.53
	OVCAR-3	−3.40
	OVCAR-4	27.16
	OVCAR-8	16.62
	NCI/ADR-RES	33.82
	SK-OV-3	3.30
Prostate cancer	DU-145	−6.52
	PC-3	28.21
Leukemia	CCRF-CEM	1.06
	HL-60(TB)	14.52
	K-562	50.22
	MOLT-4	29.50
	RPMI-8226	29.90
Renal cancer	786-0	0.38
	A498	68.14
	ACHN	10.10
	CAKI-1	29.45
	RXF393	18.97
	SN12C	−2.98
	TK-10	1.56
	UO-31	53.43
Melanoma	LOX IMVI	25.82
	M14	57.09
	MDA-MB-435	114.20
	SK-MEL-28	26.12
	SK-MEL-5	29.22
	UACC-257	14.25
CNS cancer	SF-268	2.25
	SF-295	27.88
	SF-539	0.82
	SNB-19	9.32
	SNB-75	22.17
	U251	23.41

The showed inhibition percentages are measured at a single concentration of 10 μM

Compound **13** was docked into receptor active site of both EGFR and V600E-B-RAF kinase along with their inhibitors. All the calculations were performed using MOE 2008.10 software (2008) installed on 2.0 G Core 2 Duo. The crystal structure of epidermal growth factor receptor with erlotinib (Tarceva™) (PDB code: 1M17) and the crystal structure of V600E-BRAF kinase in complex with PLX4032 (PDB code: 3OG7) were obtained from protein data bank (PDB) (Fricker, 2006; Madhusudan and Ganesan, 2004; Cockerill and lackey, 2002; Brose *et al.*, 2002; Website, 1; Bridges, 1999; Lv *et al.*, 2010; Website, 2). The automated docking program of MOE 2008.10 was used to dock compound **13** along with the inhibitors erlotinib and PLX4032 into ATP binding site of EGFR and domain of V600E-BRAF kinase, respectively. The complexes were energy-minimized with a MMFF94 force field (Halgren, 1996) till the gradient convergence 0.01 kcal/mol was reached. The binding energies of compound **13** and erlotinib docked into the active site of EGFR were −20.55 and −26.33 kcal/mol, respectively (Fig. 5). These docking studies have revealed that the imidazolidine-2,4-dione ring binds to a narrow hydrophobic pocket in the N-terminal domain of EGFR-TK where 2-carbonyl group of the imidazolidine-2,4-dione ring interacts with the backbone NH of Met-769 via a hydrogen bond, and similarly, a water (HOH-10) molecule-mediated hydrogen bonding interaction is observed between the N-1 of the imidazolidine-2,4-dione ring and the Thr-830 side chain. These interactions revealed the importance of imidazolidine-2,4-dione ring for binding and the subsequent inhibitory capacity. Compound **13** complexed with EGFR-TK in a fashion similar to erlotinib and showed the occurrence of two hydrogen bonds with Met-769 (2.99 Å) and HOH-10 (2.60 Å) mediated hydrogen bonding interaction with Thr-830 side chain (3.54 Å) and Thr-766 side chain (2.98 Å). In short, Fig. 5 demonstrates the binding model of imidazolidine-2,4-dione in the ATP binding site and the results of this molecular docking can support the postulation that our active compound may act on the same enzyme target where EGFR inhibitor acts confirming the molecular

Table 4 Calculated Lipinski's rule of five for the tested compounds

Comp. no.	UO-31[a] (% Inhibition)	Parameter					*N* violation[g]
		LogP[b]	TPSA[c]	MW[d]	*n*ON[e]	*n*OHNH[f]	
3	26.66	4.49	49.407	376.84	4	1	0
4	28.76	3.87	58.641	372.42	5	1	0
5	31.56	3.63	88.483	425.44	7	1	0
6	20.81	3.90	88.483	439.47	7	1	0
7	25.11	3.20	52.645	351.45	5	1	0
8	35.49	3.36	52.64	363.46	5	1	0
10	35.82	4.24	66.47	404.85	5	1	0
11	31.31	3.73	66.478	388.39	5	1	0
12	20.44	3.62	75.712	400.43	6	1	0
13	53.43	4.58	69.716	453.54	6	1	0
14	47.75	3.51	78.95	455.51	7	1	0
15	41.04	6.14	69.716	529.64	6	1	2
20	37.35	5.93	72.954	565.07	7	1	2

[a] Data taken from Table 1

[b] Calculated lipophilicity

[c] Total polar surface area

[d] Molecular weight

[e] Number of hydrogen bond acceptor

[f] Number of hydrogen bond donor

[g] Number of violation from Lipinski's rule of five

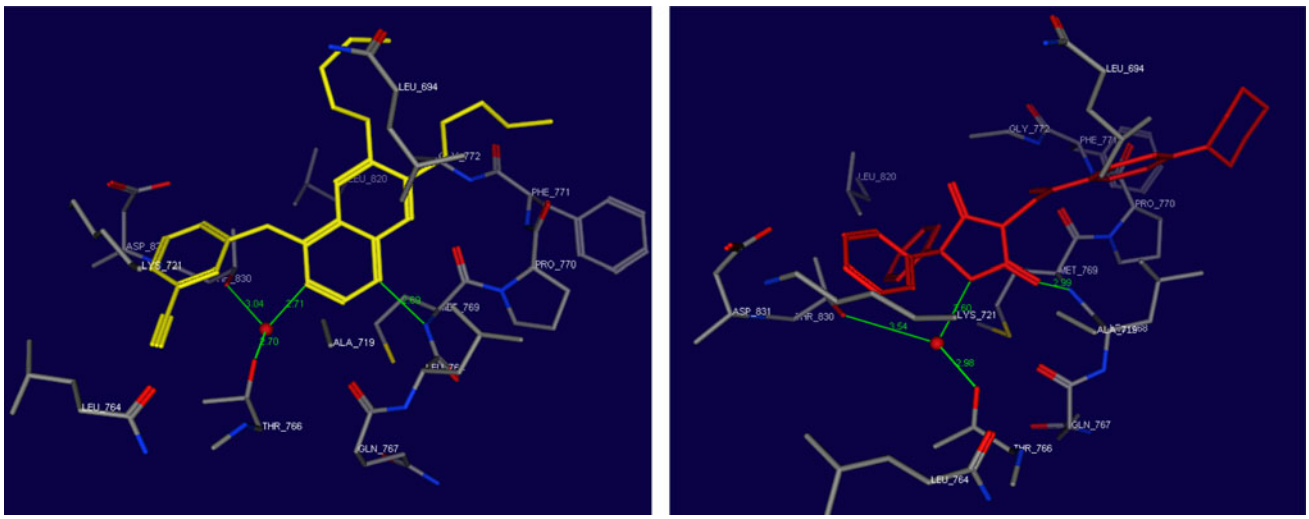

Fig. 5 Docking of the erlotinib inhibitor (*left panel*) and compounds **13** (*right panel*) into the active site of epidermal growth factor receptor. Hydrogen bonds are shown in *green* (Color figure online)

design of the reported class of antitumor agents (El-Azab *et al.*, 2010; Zuliani *et al.*, 2009; Carmi *et al.*, 2006).

On the other hand, the binding energies of compound **13** and PLX4032 docked into the active site of V600E-BRAF kinase were −33.28 and −35.11 kcal/mol, respectively (Fig. 6). The docking study has revealed that the ligand **13** has bound in the active site of one of the protomers in the protein dimer through the formation of four hydrogen bonds with Thr-529 (2.97 Å), Trp-531 (3.76 Å), Gln-530 (2.22 Å) and Cys-532 (3.11 Å). Moreover, there are two arene π–π and two arene cation interactions between the binding site and the ligand. The arene π–π interaction occurred between 5,5-diphenyl fragment and Trp-531 and Ile-463 while arene-cation interaction occurred between

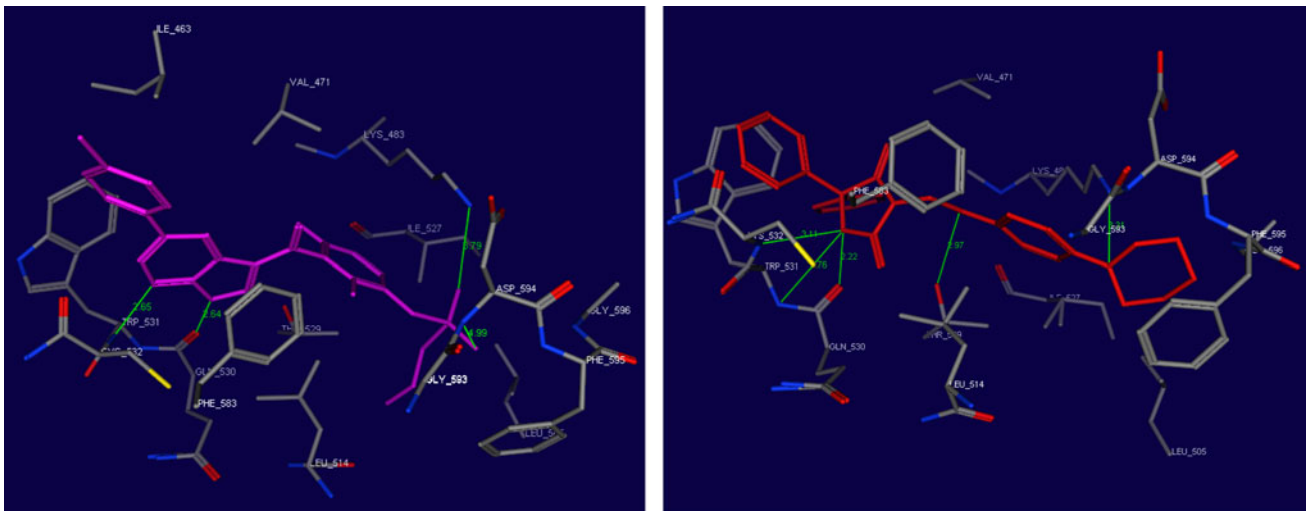

Fig. 6 Docking of the PLX4032 inhibitor (*left panel*) and compounds **13** (*right panel*) into the V600E-B-RAF kinase domain. Hydrogen bonds are shown in *green* (Color figure online)

the phenacyl fragment and Lys-483 and Gly-593 protonated amino groups. The results of this molecular docking study can support the postulation that our active compound may inhibit the growth of melanoma cell lines through inhibition of B-RAF kinase, similar to PLX4032 (Choi *et al.*, 2011).

Conclusion

The present study led to the development of promising antitumor molecules containing substituted cyclic urea (imidazolidine-2,4-dione) pharmacophore. Compound **13** exploited broad spectrum and potent antitumor activity with percentage of inhibition range of 28–114 %. The potential activity of compound **13** implies that the relative activity of these compounds is not determined only by the physicochemical properties of the substituent at the N3 position. It might only be assumed that compounds bearing a phenacyl unit are well located in the molecular target. Molecular docking into the ATP binding site of EGFR and V600E-B-RAF kinase further helps in understanding the antitumor selectivity over breast cancer MCF-7 and melanoma cancer MDA-MB-435 cell lines. Molecular docking studies further supported the inhibitory activity of **13** and further help understanding the various interactions between the ligands and enzyme active sites in detail and thereby help to design novel potent inhibitors. As evident from the experimental and calculated data, the structural features (pharmacophore) essential for the antitumor activity of this series are as follows; (1) two aromatic rings separated by an average distance; (2) a basic nitrogen atom separated from the imidazolidine-2,4-dione core by certain distance; (3) a hydrophobic moiety directly attached to the basic centre; and (4) a H-bonding acceptor (carbonyl group) attached to H-donor urea fragment. The new phenacylimidazolidine-2,4-diones prepared in this study have good physical properties that qualify them to have good pharmacokinetics and drug availability and compatible with Lipinski's rule of five. Further optimizations of antitumor and pharmacokinetic profiling of these series are currently ongoing.

Supporting information

Crystallographic data for the compound **13** have been deposited with the Cambridge Crystallographic Data Centre as the supplementary publication No. CCDC 880439. Copies of the data can be obtained, free of charge, on application to CCDC, 12 Union Road, Cambridge CB2 1EZ, UK, Fax: +44-1223-336033 or e-mail: deposit@ccdc.cam.ac.uk.

Acknowledgments The authors extend their appreciation to the Deanship of Scientific Research at King Saud University for funding the study through the research group project No. RGP-VPP-163. The authors would like to express their gratitude and thanks to the National Cancer Institute (NCI), Bethesda, MD, USA, http://dtp.cancer.gov/ for doing the antitumor testing of the new compounds.

References

Abdel-Aziz AA-M (2007) Novel and versatile methodology for synthesis of cyclic imides and evaluation of their cytotoxic, DNA binding, apoptotic inducing activities and molecular modeling study. Eur J Med Chem 42:614–626

Abdel-Aziz AA-M, Al-Omar MA, El-Azab AS, Kunieda T (2010) Conformational preferences of sterically congested 2-imidazolidinone using X-ray analysis and computational studies. Part 1:

Trans-1-acetyl-4,5-di-tert-butyl-2-imidazolidinone. J Mol Struct 969:145–154

Abdel-Aziz AA-M, ElTahir KEH, Asiri YA (2011) Synthesis, anti-inflammatory activity and COX-1/COX-2 inhibition of novel substituted cyclic imides. Part 1: molecular docking study. Eur J Med Chem 46:1648–1655

Abdel-Aziz AA-M, El-Azab AS, El-Subbagh HI, Al-Obaid AM, Alanazi AM, Al-Omar MA (2012) Design, synthesis, single-crystal and preliminary antitumor activity of novel arenesulfonylimidazolidin-2-ones. Bioorg Med Chem Lett 22:2008–2014

Al-Obaid AM, Abdel-Hamide SG, El-Kashef HA, Abdel-Aziz AA-M, El-Azab AS, Al-Khamees HA, El-Subbagh HI (2009) Substituted quinazolines, part 3. Synthesis, in vitro antitumor activity and molecular modeling study of certain 2-thieno-4(3H)-quinazolinone analogs. Eur J Med Chem 44:2379–2391

Al-Omary FA, Abou-Zeid LA, Nagi MN, Habib SE, Abdel-Aziz AA-M, El-Azab AS, Abdel-Hamide SG, Al-Omar MA, Al-Obaid AM, El-Subbagh HI (2010) Non-classical antifolates. Part 2: synthesis, biological evaluation, and molecular modeling study of some new 2,6-substituted-quinazolin-4-ones. Bioorg Med Chem 18:2849–2863

Ananda KCS, Benaka PSB, Vinaya K, Chandrappa S, Thimmegowda NR, Kumar YC, Swarup S, Rangappa KS (2009) Synthesis and in vitro antiproliferative activity of novel 1-benzhydrylpiperazine derivatives against human cancer cell lines. Eur J Med Chem 44:1223–1229

Avendaño C, Menéndez JC (2008) Medicinal chemistry of anticancer drugs. Elsevier, Amsterdam, pp 1–459

Bakalova A, Buyukliev R, Tcholakova I, Momekov G, Konstantinov S, Karaivanova M (2003) Synthesis, physicochemical investigation and cytotoxic activity of new Pt(II) complexes with hydantoin ligands. Eur J Med Chem 38:627–632

Basappa AK, Nanjunda SS, Sugahara K, Rangappa KS (2009) Anti-tumor and anti-angiogenic activity of novel hydantoin derivatives: inhibition of VEGF secretion in liver metastatic osteosarcoma cells. Bioorg Med Chem 17:4928–4934

Boyd MR, Paull KD (1995) Some practical considerations and applications of the National Cancer Institute in vitro anticancer drug discovery screen. Drug Dev Res 34:91–109

Bridges AJ (1999) The rationale and strategy used to develop a series of highly potent, irreversible, inhibitors of the epidermal growth factor receptor family of tyrosine kinases. Curr Med Chem 6:825–843

Bridges AJ, Zhou H, Cody DR, Rewcastle GW, McMichael A, Showalter HD, Fry DW, Kraker AJ, Denny WA (1996) Tyrosine kinase inhibitors. 8. An unusually steep structure-activity relationship for analogues of 4-(3-bromoanilino)-6,7-dimethoxyquinazoline (PD 153035), a potent inhibitor of the epidermal growth factor receptor. J Med Chem 39:267–276

Brose MS, Volpe P, Feldman M, Kumar M, Rishi I, Gerrero R, Einhorn E, Herlyn M, Minna J, Nicholson A, Roth JA, Albelda SM, Davies H, Cox C, Brignell G, Stephens P, Futreal PA, Wooster R, Stratton MR, Weber BL (2002) BRAF and RAS mutations in human lung cancer and melanoma. Cancer Res 62:6997–7000

Carmi C, Cavazzoni A, Zuliani V, Lodola A, Bordi F, Plazzi PV, Alfieri RR, Petronini PG, Mor M (2006) 5-benzylidene-hydantoins as new EGFR inhibitors with antiproliferative activity. Bioorg Med Chem Lett 16:4021–4025

Cavazzoni A, Alfieri RR, Carmi C, Zuliani V, Galetti M, Fumarola C, Frazzi R, Bonelli M, Bordi F, Lodola A, Mor M, Petronini PG (2008) Dual mechanisms of action of the 5-benzylidene-hydantoin UPR1024 on lung cancer cell lines. Mol Cancer Ther 7:361–370

Choi WK, El-Gamal MI, Choi HS, Baek D, Oh CH (2011) New diarylureas and diarylamides containing 1,3,4-triarylpyrazole scaffold: synthesis, antiproliferative evaluation against melanoma cell lines, ERK kinase inhibition, and molecular docking studies. Eur J Med Chem 46:5754–5762

Choo HY, Choi S, Jung SH, Koh HY, Pae AN (2003) The 3D-QSAR study of antitumor arylsulfonylimidazolidinone derivatives by CoMFA and CoMSIA. Bioorg Med Chem 11:4585–4589

Clark DE, Pickett SD (2000) Computational methods for the prediction of 'drug-likeness'. Drug Discov Today 5:49–58

Cockerill GS, Lackey KE (2002) Small molecule inhibitors of the class 1 receptor tyrosine kinase family. Curr Top Med Chem 2:1001–1010

Dumbris SM, Díaz DJ, McElwee-White L (2009) Preparation of hydantoins by catalytic oxidative carbonylation of alpha-amino amides. J Org Chem 74:8862–8865

Eckhardt S (2002) Recent progress in the development of anti cancer agents. Curr Med Chem 2:419–439

El-Ayaan U, Abdel-Aziz AA-M, Al-Shihry S (2007) Solvatochromism, DNA binding, antitumor activity and molecular modeling study of mixed-ligand copper(II) complexes containing the bulky ligand: bis[*N*-(p-tolyl)imino]acenaphthene. Eur J Med Chem 42:1325–1333

El-Azab AS, Al-Omar MA, Abdel-Aziz AA-M, Abdel-Aziz NI, El-Sayed MA-A, Aleisa AM, Sayed-Ahmed MM, Abdel-Hamide SG (2010) Design, synthesis and biological evaluation of novel quinazoline derivatives as potential antitumor agents: molecular docking study. Eur J Med Chem 45:4188–4198

El-Deeb IM, Bayoumi SM, El-Sherbeny MA, Abdel-Aziz AA-M (2010) Synthesis and antitumor evaluation of novel cyclic arylsulfonylureas: ADME-T and pharmacophore prediction. Eur J Med Chem 45:2516–2530

El-Sayed MA-A, Abdel-Aziz NI, Abdel-Aziz AA-M, El-Azab AS, Asiri YA, ElTahir KEH (2011) Design, synthesis, and biological evaluation of substituted hydrazone and pyrazole derivatives as selective COX-2 inhibitors: molecular docking study. Bioorg Med Chem 19:3416–3424

El-Sayed MA-A, Abdel-Aziz NI, Abdel-Aziz AA-M, El-Azab AS, ElTahir KEH (2012) Synthesis, biological evaluation and molecular modeling study of pyrazole and pyrazoline derivatives as selective COX-2 inhibitors and anti-inflammatory agents. Part 2. Bioorg Med Chem 20:3306–3316

El-Sherbeny MA, Abdel-Aziz AA-M, Ahmed MA (2010) Synthesis and antitumor evaluation of novel diarylsulfonylurea derivatives: molecular modeling applications. Eur J Med Chem 45:689–697

El-Zanfally S, Khalifa M, Abou-Zeid YM (1968) New compounds: derivatives of some imido compounds likely to possess therapuetic acitivy. J Pharm Sci 57:2176–2179

Fricker J (2006) Tyrosine kinase inhibitors: the next generation. Lancet Oncol 7:621

Goda FE, Abdel-Aziz AA-M, Ghoneim HA (2005) Synthesis and biological evaluation of novel 6-nitro-5-substituted aminoquinolines as local anesthetic and anti-arrhythmic agents: molecular modeling study. Bioorg Med Chem 13:3175–3183

Grever MR, Schepartz SA, Chabner BA (1992) The National Cancer Institute: cancer drug discovery and development program. Semin Oncol 19:622–638

Halgren TA (1996) Merck molecular force field. 1. Basis, form, scope, parameterization, and performance of MMFF94. J Comput Chem 17:490–519

Hmuda SF, Trisovic NP, Valentic NV, Uscumlic GS (2011) Solvent effects on the structure–property relationship of some potentially pharmacologically active 3-(4-substituted benzyl)-5-ethyl-5-phenyl- and 3-(4-substituted benzyl)-5,5-diphenylhydantoins. J Solut Chem 40:307–319

Khanfar MA, El Sayed KA (2010) Phenylmethylene hydantoins as prostate cancer invasion and migration inhibitors. CoMFA approach and QSAR analysis. Eur J Med Chem 45:5397–5405

Kim IW, Lee CK, Kim HS, Jung SH (2003) Importance of sulfonylimidazolidinone motif of 4-phenyl-1-arylsulfonylimidazolidinones for their cytotoxicity: synthesis of 2-benzoyl-4-phenyl[1,2,5]thiazolidine-1,1-dioxides and their cytotoxcity. Arch Pharm Res 26:9–14

Lee HS, Park KL, Choi SU, Lee CO, Jung SH (2000) Effect of substituents on benzenesulfonyl motif of 4-phenyl-1-arylsulfonylimidazolidinones for their cytotoxicity. Arch Pharm Res 23:579–584

Lee CW, Hong DH, Han SB, Jung SH, Kim HC, Fine RL, Lee SH, Kim HM (2002) A novel stereo-selective sulfonylurea, 1-[1-(4-aminobenzoyl)-2,3-dihydro-1H-indol-6-sulfonyl]-4-phenyl-imidazolidin-2-one, has antitumor efficacy in in vitro and in vivo tumor models. Biochem Pharmacol 64:473–480

Lipinski CA, Lombardo F, Dominy BW, Feeney PJ (2001) Experimental and computational approaches to estimate solubility and permeability in drug discovery and development settings. Adv Drug Deliv Rev 46:3–26

Lv PC, Wang KR, Li QS, Chen J, Sun J, Zhu HL (2010) Design, synthesis and biological evaluation of chrysin long-chain derivatives as potential anticancer agents. Bioorg Med Chem 18:1117–1123

Madhusudan S, Ganesan TS (2004) Tyrosine kinase inhibitors in cancer therapy. Clin Biochem 37:618–635

MOE 2008. 10 of Chemical Computing Group Inc

Monks A, Schudiero D, Skehan P, Shoemaker R, Paull K, Vistica D, Hose C, Langley J, Cronise P, Vaigro-Wolff A, Gray-Goodrich M, Campbell H, Mayo J, Boyd M (1991) Feasibility of a high-flux anticancer drug screen using a diverse panel of cultured human tumor cell lines. J Natl Cancer Inst 83:757–766

Ooms F, Wouters J, Oscari O, Happaerts T, Bouchard G, Carrupt PA, Testa B, Lambert DM (2002) Exploration of the pharmacophore of 3-alkyl-5-arylimidazolidinediones as new CB(1) cannabinoid receptor ligands and potential antagonists: synthesis, lipophilicity, affinity, and molecular modeling. J Med Chem 45:1748–1756

Park Choo HY, Lim JS, Kam Y, Kim SY, Lee J (2001) A comparative study of quantitative structure activity relationship methods based on antitumor diarylsulfonylureas. Eur J Med Chem 36: 829–836

Penthala NR, Yerramreddy TR, Crooks PA (2011) Synthesis and in vitro screening of novel *N*-benzyl aplysinopsin analogs as potential anticancer agents. Bioorg Med Chem Lett 21: 1411–1413

Peretto I, Fossati C, Giardina GA, Giardini A, Guala M, La Porta E, Petrillo P, Radaelli S, Radice L, Raveglia LF, Santoro E, Scudellaro R, Scarpitta F, Cerri A, Menegon S, Dondio GM, Rizzi A, Armani E, Amari G, Civelli M, Villetti G, Patacchini R, Bergamaschi M, Bassani F, Delcanale M, Imbimbo BP (2007) Discovery of diaryl imidazolidin-2-one derivatives, a novel class of muscarinic M3 selective antagonists (Part 2). J Med Chem 50:1693–1697

Thirupathi RY, Narsimha RP, Koduru S, Damodaran C, Crooks PA (2010) Aplysinopsin analogs: synthesis and anti-proliferative activity of substituted (Z)-5-(*N*-benzylindol-3-ylmethylene)imidazolidine-2,4-diones. Bioorg Med Chem 18:3570–3574

Traxler P, Bold G, Frei J, Lang M, Lydon N, Mett H, Buchdunger E, Meyer T, Mueller M, Furet P (1997) Use of a pharmacophore model for the design of EGF-R tyrosine kinase inhibitors: 4-(phenylamino)pyrazolo[3,4-d]pyrimidines. J Med Chem 40: 3601–3602

Trišović N, Božić B, Obradović A, Stefanović O, Marković S, Čomić L, Božić B, Uŝcumlić G (2011) Structure–activity relationships of 3-substituted-5,5-diphenylhydantoins as potential antiproliferative and antimicrobial agents. J Serbian Chem Soc 76:1597–1606

Varmus H (2006) The new era in cancer research. Science 312: 1162–1165

Wissner A, Berger DM, Boschelli DH, Floyd MB Jr, Greenberger LM, Gruber BC, Johnson BD, Mamuya N, Nilakantan R, Reich MF, Shen R, Tsou HR, Upeslacis E, Wang YF, Wu B, Ye F, Zhang N (2000) 4-Anilino-6,7-dialkoxyquinoline-3-carbonitrile inhibitors of epidermal growth factor receptor kinase and their bioisosteric relationship to the 4-anilino-6,7-dialkoxyquinazoline inhibitors. J Med Chem 43:3244–3256

Website 1: http://www.rcsb.org/pdb/explore.do?structureId=1M17 (Deposition: 2002-06-17). Accessed 2 Oct 2012

Website 2: http://www.rcsb.org/pdb/explore/explore.do?structureId=3OG7 (Deposition: 2010-08-16). Accessed 7 Oct 2012

Zuliani V, Carmi C, Rivara M, Fantini M, Lodola A, Vacondio F, Bordi F, Plazzi PV, Cavazzoni A, Galetti M, Alfieri RR, Petronini PG, Mor M (2009) 5-Benzylidene-hydantoins: synthesis and antiproliferative activity on A549 lung cancer cell line. Eur J Med Chem 44:3471–3479